

1 **Factors influencing taper failure of modular revision hip** 2 **stems**

3 Krull A. *, Morlock M.M.*, Bishop N.E. **

4 *TUHH – Hamburg University of Technology
5 Institute of Biomechanics
6 Denickestrasse 15
7 21073 Hamburg
8 Germany

9 **HAW Hamburg University of Applied Science
10 Fakultät Life Science
11 Department Medizintechnik
12 Ulmenliet 20
13 21033 Hamburg
14 Germany

15

16 **Corresponding author:**

17 Annika Krull
18 Telephone: +49 40 428783157
19 annika.krull@tuhh.de

20 **Main text:** 4438 words

21 **Abstract:** 241 words

22 **Number of figures and tables:** 8 figures, 1 table

23

24 **Abstract**

25 Stem modularity of revision hip implant systems offers the advantage of the restoration of
26 individual patient geometry but introduces additional interfaces, which are subjected to
27 repetitive bending loading and have a propensity for fretting corrosion. The male stem taper
28 is the weakest part of the modular junction due to its reduced cross section compared to the
29 outside diameter of the stem. Taper fractures can be the consequence of overloading in
30 combination with corrosion. The purpose of this study was to assess the influence of implant
31 design factors, patient factors, and surgical factors on the risk of taper failure of the modular
32 junction of revision stems.

33 An analytical bending model was used to estimate the strength of the taper connection for
34 pristine, fatigued and corroded conditions. Additionally, a finite element contact model of
35 the taper connection was developed to assess the relative motion and potential for surface
36 damage at the taper interface under physiological loading for varying assembly and design
37 parameters.

38 Increasing the male taper diameter was shown to be the most effective means for increasing
39 taper strength but would require a concurrent increase in the outer implant diameter to
40 limit a greater risk of total surface damage for a thinner female taper wall. Increasing the
41 assembly force decreases the total surface damage but not local magnitudes, which are
42 probably responsible for crack initiation. It is suggested that in unfavourable loading
43 conditions a monobloc implant system will reduce the risk of failure.

44 **Keywords**

45 Hip revision, taper junction, fracture, corrosion, fatigue, strength, titanium, finite element
46 model, surface damage

47 **Highlights**

- 48 • Simple stress analysis demonstrates the limited mechanical safety factor at the stem
49 taper junction of modular hip revision systems, indicating that patient loading due to
50 activity and/or weight should be limited.
- 51 • Increasing the taper junction diameter increases strength - but contact analysis
52 demonstrated an increase in the risk of total surface damage unless the outer diameter is
53 also increased.
- 54 • Contact analysis demonstrated that increasing the assembly force decreases the total
55 surface damage but local magnitudes can still be critical.

56 **Introduction**

57 The numbers of revision of both primary and revision hip implantations are steadily
58 increasing [1]. Revision rates for first revision at 10 years in national arthroplasty registries
59 between 3 % and 20 % are reported [2-10]. Revision rates of primary implantations in the
60 same registries are much lower (between 2 % and 4 % if metal-on-metal bearing articulation
61 are omitted) [6,64]. Revision implantation is more challenging than primary procedures as
62 bone stock has often been lost due to stress shielding and the operative removal of the

63 primary implant and the cement mantle, mostly in the proximal region. In anticipation of
64 further revision procedures revision stems are typically uncemented, and are therefore
65 made of titanium alloys which are compatible with bone ingrowth. They are anchored by
66 press-fit in the distal femur. This necessitates a femoral stem that is longer for a revision
67 implant than for a primary stem [11]. Modularity has found widespread application in
68 revision femoral stems as it allows for intra-operative adaptation to the conditions of the
69 femoral bone. Modular systems also require less inventory than monobloc (non-modular)
70 systems. Modular systems incorporate a taper junction between prosthesis neck component
71 and stem, generally located in the proximal third of the implant, allowing the distal stem to
72 be implanted and the proximal neck component to be fitted to the anatomy and assembled
73 subsequently.

74 Failure of modular connections has been reported to occur by dislocation, corrosion and
75 fracture [12–18]. Failure by fracture of a revision stem is reported at rates of 0.9 % to 3.6 %
76 [4]. Fracture is induced mechanically by fretting, involving the repetitive mechanical
77 disruption of the protective oxide surface layer of the bulk metal due to oscillating relative
78 motion between two surfaces in contact. By definition the amplitude is smaller than the
79 width of nominal contact area. The resulting damage can occur due to wear, fatigue or
80 corrosion. The process of passive oxide film removal due to fretting, followed by corrosion, is
81 called “fretting corrosion”. Modular junctions in revision stems are subject to high bending
82 moments, due to their offset (lever arm) from the joint force vector, especially in situations
83 without proximal bone support. Patient anatomy and body weight also influence bending
84 loading of the taper [14,16,18–20]. The diameter of the intramedullary canal limits the
85 maximum diameter of the stem that can be implanted. Increased loading cannot always be
86 compensated by implant dimensions, leading to limited flexural strength [14,17–19,23,24].
87 This also applies to the taper dimensions, which are limited by the outside diameter of the
88 implant. Failure has also been documented for the stem-head taper junction, particularly in
89 association with the re-introduction of large diameter metal-on-metal joints, which can
90 generate increased joint friction moments [13–18].

91 Failure of revision stems is generally due to fatigue fracture [24,25]. Fracture of an implant
92 occurs when stresses exceed the material strength. Pristine components have the greatest
93 strength, which decreases with fatigue loading and corrosion. Higher assembly forces have

94 the potential to reduce fretting by increasing the press-fit [26–28]. A parametric analysis of
95 the major factors responsible for prosthesis failure is not available.

96 The purpose of this study was therefore to investigate the influence of joint loading, stem
97 taper geometry, material characteristics and assembly force on potential taper failure of
98 modular revision hip stems.

99 **Materials and Methods**

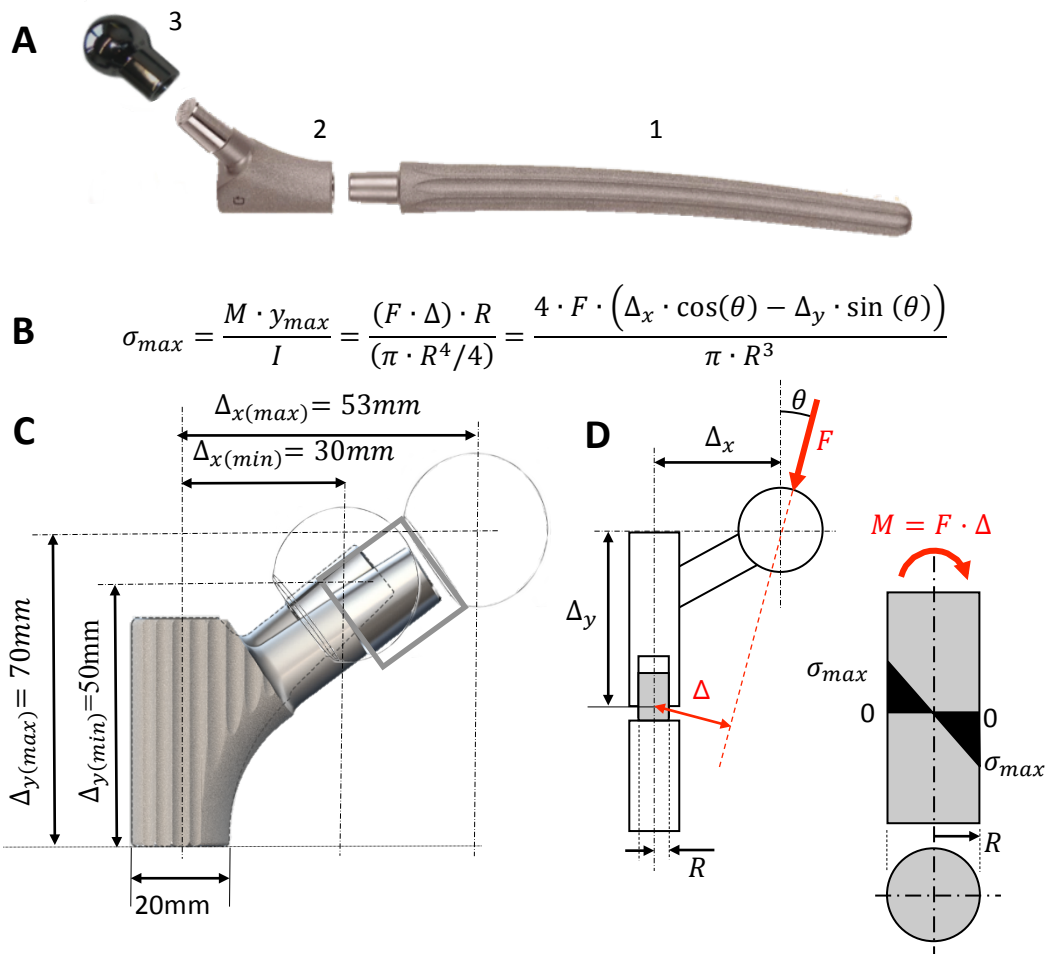
100 Stress magnitudes were assessed analytically for different realistic implant geometries and
101 patient loading scenarios, and related to the strength of the material in various states of
102 degradation by fatigue and corrosion. The influence of the modular taper design and
103 assembly force on degradation of the material by surface damage were also analysed, using
104 finite element (FE) analysis. For validation of the analytical and numerical models,
105 experimental determination of the fracture load, seating depth and gap opening at the taper
106 connection under different assembly loads were performed.

107 A clinically successful modular THA revision prosthesis system (MRP, Peter Brehm GmbH,
108 Germany) was used as basis for the analysis [22]. The femoral implant of the MRP consists of
109 a distal stem and a proximal neck piece (Figure 1A). For this study a neck piece with a CCD
110 angle of 130 ° was used (Figure 1C). Both components are made from Ti6Al4V alloy (Ti) and
111 have an outside diameter of 20 mm. The components are joined by a taper connection with
112 a diameter of ~12 mm for the male taper, a taper angle of 1.4 ° (from the mid-axis) and a
113 contact length between male and female components of 19.5 mm when assembled. The
114 lateralised proximal neck piece in combination with an L4 prosthesis head (+16 mm)
115 produces a horizontal offset of 53 mm. This was investigated as a worst-case loading
116 scenario of the taper connection (“high offset”; Figure 1C), since this results in the highest
117 bending moment possible at the modular junction. This combination is not approved by the
118 manufacturer but is used clinically. For comparison a “short” (-5 mm) head with a standard
119 neck piece producing a horizontal offset of 30 mm was also investigated (“low offset”; Figure
120 1C).

121 ***Analytical***

122 A simple beam bending model was used to calculate the maximum bending stresses σ_{max} for
123 the outside surface of the male taper of the distal stem, according to joint loading and
124 implant geometry (Figure 1B). The joint load was assumed to act through the centre of the

125 prosthesis head, in the plane of the implant and at an angle θ to the vertical implant axis.
 126 The bending moment M acting around the centre of the male taper of the distal stem, at the
 127 level of the open end of the proximal neck piece, was calculated from the joint force vector
 128 and its distance Δ from this point (Figure 1D). The radius R of the male taper of the distal
 129 stem at this point was varied. Peak joint forces F measured in vivo during walking and
 130 stumbling for a light (60 kg) and a heavy patient (120 kg) [29] were applied. Calculated
 131 stresses were compared with the strength of pristine Ti6Al4V ($\hat{\sigma}_{pristine} = 1000 \text{ MPa}$) [53], a
 132 fatigued material at 10^7 cycles ($\hat{\sigma}_{fatigue} = 750 \text{ MPa}$) [30] and a severely corroded
 133 material ($\hat{\sigma}_{corrosion} = 200 \text{ MPa}$) [30].
 134 The analysis assumes linear bending theory. Stresses due to the axial and shear force
 135 components are neglected as they are relatively small [63]. It was assumed that there was
 136 no bony support of the proximal neck piece.



137
 138 **Figure 1:** A: The femoral component consisting of distal stem (1), proximal neck piece (2),
 139 prosthesis head (3);

140 **B:** Equation for the calculation of maximum bending stress σ_{max} at the male taper
 141 of the distal stem. M is the applied bending moment, y_{max} the maximum distance
 142 from the neutral plane, I is the second moment of area around the bending axis, F is
 143 the joint force, Δ is the perpendicular distance from the force vector to the taper, θ
 144 is the angle of the joint force to the vertical implant axis and R is the radius of the
 145 male taper at the level of the open end of the proximal taper (circular cross
 146 section);

147 **C:** “High” and “low” offset geometries investigated;

148 **D:** Representation of the male taper stressed in bending due to the joint force and
 149 its offset from the taper. The moment M acting around the taper connection is
 150 derived from the joint force F acting at an offset Δ from the taper.

151 **Numerical**

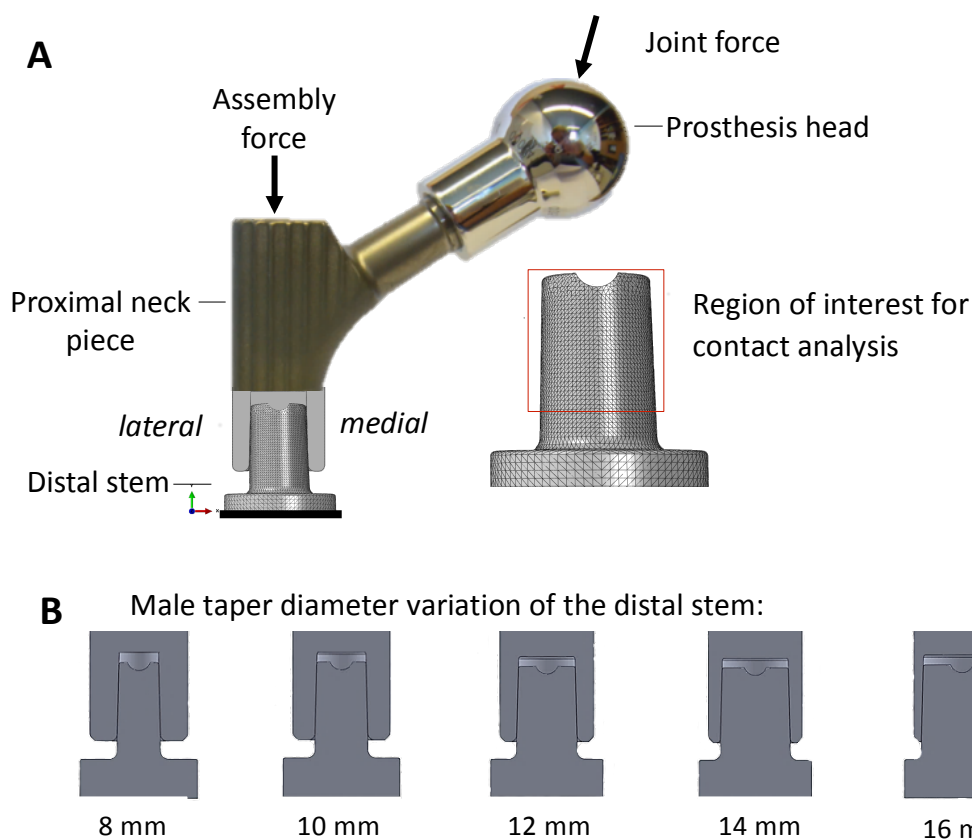
152 Fretting damage can occur when small relative motions between two interface surfaces in
 153 contact occur [21,26], which abrade the protective oxide layers. In a fluid environment,
 154 metal ions can leave the bare metal surface, which is known as fretting corrosion [31]. In
 155 titanium alloys this leads to a roughened surface that causes stress concentrations as sites of
 156 crack nucleation [32].

157 A finite element model of the stem taper junction was generated (Abaqus 6.14, Dassault
 158 Systèmes, France) based on CAD data of the MRP-System (Figure 2A). Contact analysis of the
 159 taper interface was implemented to investigate mechanical and design factors potentially
 160 influencing fretting damage. Linearly elastic, homogeneous, isotropic material properties for
 161 the titanium alloy Ti6Al4V Ti were used ($E=113.8$ GPa; $\nu=0.34$). The friction coefficient for
 162 contact of the alloy surfaces was set to $\mu=0.35$ [33,34].

163 A mesh convergence analysis resulted in a suitable element size of 0.8 mm on the contact
 164 surface of the taper junction (proximal neck piece and distal stem), resulting in
 165 105,837 elements for the distal stem and changes of less than 2 % in gap opening and
 166 seating depth between mesh refinements. Relative shear interface motion and contact
 167 pressure were sampled at each node of the surface of the male taper. Assembly forces were
 168 varied between 0.5 kN and 40.0 kN, representing very low intraoperative values and very
 169 high laboratory values, respectively. Physiological joint loading for a walking cycle of a 75 kg
 170 patient was applied, according to in-vivo measurements in joint replacement patients [29].

171 Relative shear interface motion and pressure at each node were multiplied to obtain a factor
 172 representing relative surface damage for ten equally spaced time intervals of the loading
 173 cycle (based on Archard's law [35,36]). Total surface damage was determined by summing
 174 over all nodes and all time intervals.

175 The influence of prosthesis design was investigated by the variation of the male taper
 176 diameter between 8 mm and 16 mm, with the outside diameter of the implant maintained
 177 at 20.0 mm, the length of contact at 19.5 mm and the taper angle at 1.4° (Figure 2B). For
 178 this parametric analysis an assembly force of 11.0 kN was applied, followed by the peak joint
 179 force in a gait cycle [29].



180

181 **Figure 2:** A: The numerical model (grey) with loading applied to represent the applied forces
 182 shown;

183 B: Variation of the diameter of the male stem taper between 8 mm and 16 mm.
 184 12 mm represents the clinically available implant.

185 **Validation**

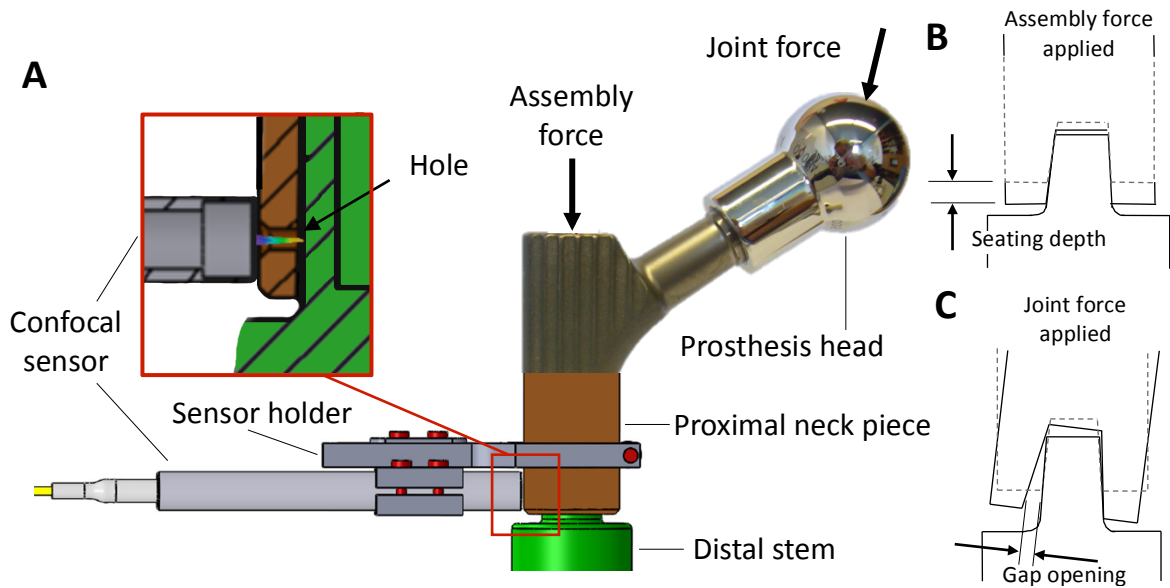
186 For experimental validation of the analytical bending stress model, the fracture load of the
 187 modular implant was determined and compared with the analytical prediction. The proximal

188 neck piece was assembled under 9.0 kN on a replica of the distal stem piece (produced by
189 the implant manufacturer) using a materials testing machine (Zwick Z010, Zwick GmbH &
190 Co.KG, Germany; in accordance with ISO 7206-10; 0.04 mm/s). The prosthesis head was then
191 loaded vertically until fracture of the taper (n=3). The peak force was recorded.

192 For experimental validation of the FE model, the opening of the gap at the taper interface
193 was measured in the radial direction at the lateral side using a chromatic confocal sensor (DT
194 IFS 2403-1.5, Micro-Epsilon Messtechnik GmbH, Germany; measurement range: 1.5 mm,
195 resolution 60 nm) mounted on the outside surface on an aluminium clamp (Figure 3A). The
196 change in distance to the male taper surface was measured through a 1.5 mm diameter hole
197 drilled through the proximal neck piece at the lower edge of the lateral side. Measurements
198 were repeated three times.

199 The two prosthesis components were assembled quasi-statically at 0.04 mm/s (ISO 7206-10)
200 with forces of 0.5, 5.0 and 9.0 kN, along the taper axis using a materials testing machine
201 (Zwick Z010, Zwick GmbH & Co.KG, Germany). After assembly, a joint force of 0.5, 1.5 or
202 2.5 kN was applied under quasistatic displacement (0.04mm/s) to the prosthetic head with a
203 horizontal offset of 53 mm along an axis parallel to the stem taper axis (0.04 mm/s). The 2.5
204 kN joint force reflects magnitudes measured for gait [29]. The seating depth (Figure 3B) after
205 assembly and the gap opening (Figure 3C) at the taper junction between the proximal neck
206 piece and the distal stem at the lateral side of the female taper opening were measured.

207 The seating depth was derived from the difference in axial position of the proximal neck
208 piece on the distal stem component measured before and after assembly using a coordinate
209 measurement machine (Mitutoyo BHN 305; Mitutoyo Deutschland GmbH, Germany;
210 accuracy 2 μm). One measurement was performed for each assembly force (n=3). No joint
211 force was applied during these tests.



212

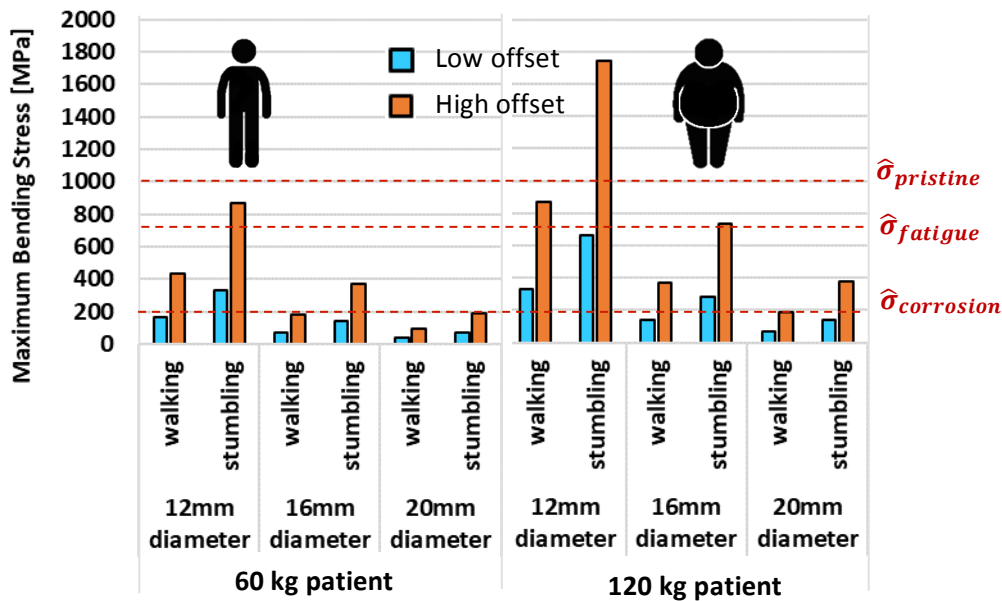
213 **Figure 3: A:** Gap opening at the taper junction was measured through a small hole in the
 214 proximal neck piece using a confocal sensor mounted on the proximal neck piece;
 215 **B:** Illustration of the seating depth between the proximal neck piece and the distal
 216 stem due to an applied assembly force;
 217 **C:** Illustration of the gap opening between the proximal neck piece and the distal
 218 stem due to joint force.

219 **Results**

220 **Analytical**

221 The bending model predicted taper failure for the standard taper diameter (12 mm) for the
 222 pristine material condition only under high offset in a heavy patient under a stumbling load
 223 (Figure 4). The same implant configuration failed for a light patient stumbling or a heavy
 224 patient walking for the fatigued material after 10^7 loading cycles. Increasing the male taper
 225 diameter to 16 mm prevented failure of the pristine or fatigued components for any patient,
 226 geometry or loading (Figure 4).

227 The corroded material led to failure for almost any condition for the standard diameter
 228 taper. Increasing the taper diameter to 20 mm, which would correspond to a monobloc
 229 implant of this dimension, protected against failure in almost all conditions, excepting a
 230 heavy patient stumbling with a high offset implant.

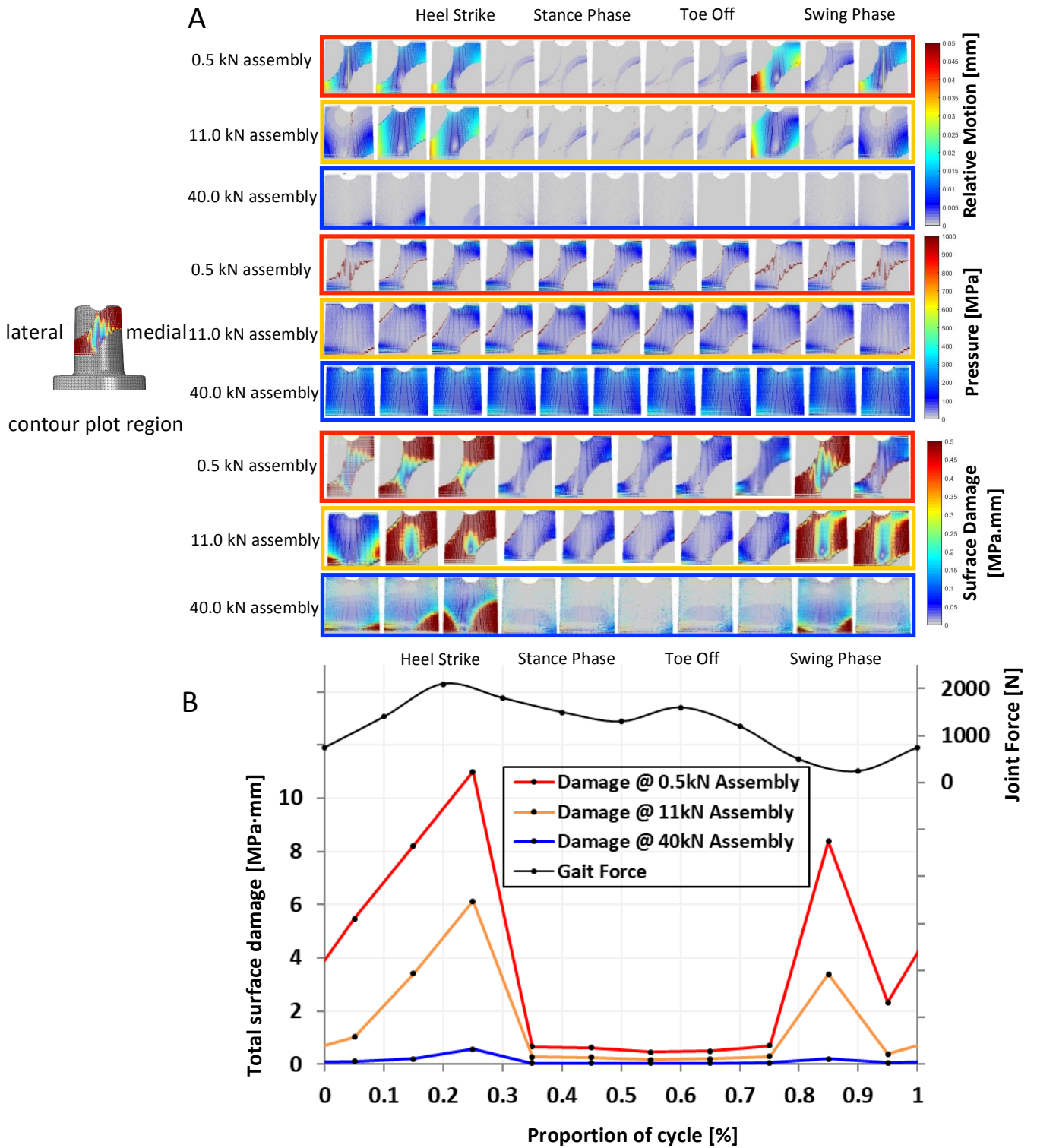


231

232 **Figure 4:** Peak bending stresses for the male taper of the distal stem for low (60 kg) and high
 233 patient mass (120 kg), low (30 mm) and high offset (53 mm) and varying diameters
 234 of the male stem taper (12 mm, 16 mm and 20 mm). Failure stresses of the
 235 different material conditions (pristine, fatigue and corrosion) are indicated.

236 **Finite element model**

237 An increase in contact pressure and contact area as well as a decrease in relative motion
 238 under joint loading were found for increasing assembly force (Figure 5A, Table 1). Gap
 239 opening was observed in the proximal-lateral and distal-medial regions and was reduced
 240 with increasing assembly force (Figure 5A, Table 1). The same peak magnitude of the total
 241 surface damage was observed for all assembly forces, despite decreasing relative motion for
 242 higher assembly forces, due to the increased contact pressure (Table 1). Peak total surface
 243 damage was observed in distal-lateral and proximal-medial regions for low assembly forces
 244 (0.5 kN), over the whole of the lateral and medial surfaces for increased assembly force
 245 (11.0 kN) and in the distal regions of the lateral and medial surfaces for very high assembly
 246 loads (40.0 kN) (Figure 5A). The greatest total surface damage was observed for the periods
 247 of the joint loading cycle with the highest rates of loading and unloading (heel strike and toe
 248 off; Figure 5B). The total surface damage integrated over the taper surface for a whole gait
 249 cycle decreased with increasing assembly force: 4.33 MPa·mm, 1.73 MPa·mm and
 250 0.14 MPa·mm for 0.5 kN, 11.0 kN and 40.0 kN, respectively (Figure 5B, Table 1).



251

252 **Figure 5 : A:** Contour plots of the relative motion, pressure and relative surface damage for
 253 each tenth of the gait cycle for three assembly forces (the colours of the frames
 254 reflects the different assembly forces and corresponds to the colours in part B of
 255 this figure);

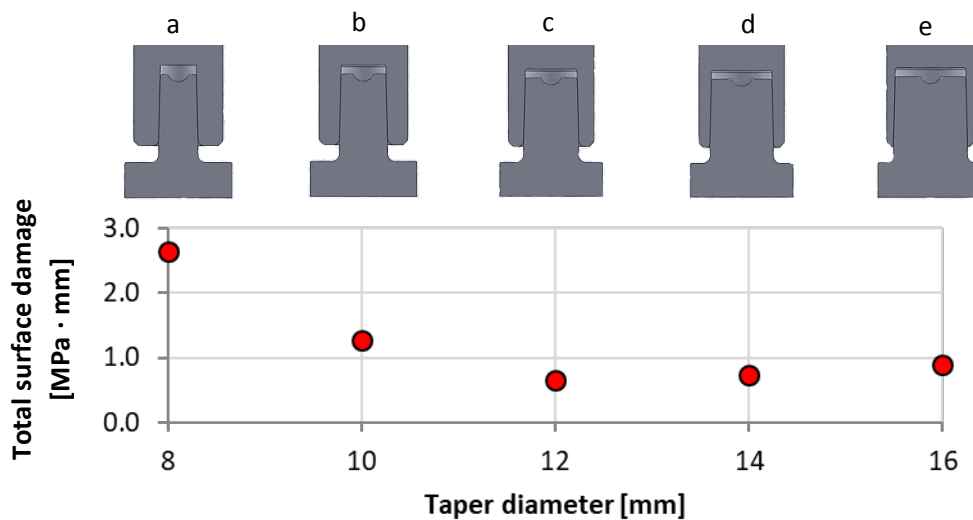
256 **B:** Total surface damage for the entire surface for each tenth of the gait cycle,
 257 starting and ending with the swing phase of the leg.

258

259 **Table 1:** Maximum relative motion [mm], contact pressure [MPa], gap opening [mm] during
 260 a gait cycle, and total surface damage [MPa·mm] integrated over the whole gait
 261 cycle for the different assembly forces [kN] from the FE analysis.

Assembly force [kN]	Relative motion [mm]	Contact pressure [MPa]	Gap opening [mm]	Total surface damage integrated over the whole gait cycle [MPa·mm]
0.5	0.01200	92.24	0.047	4.33
11.0	0.00540	128.93	0.026	1.73
40.0	0.00072	205.73	0.003	0.14

262 The total surface damage of the different taper diameters (assembly force 11.0 kN and peak
 263 force of physiological gait loading) showed the smallest magnitude for condition “c” (Figure
 264 6), which is the design used clinically.



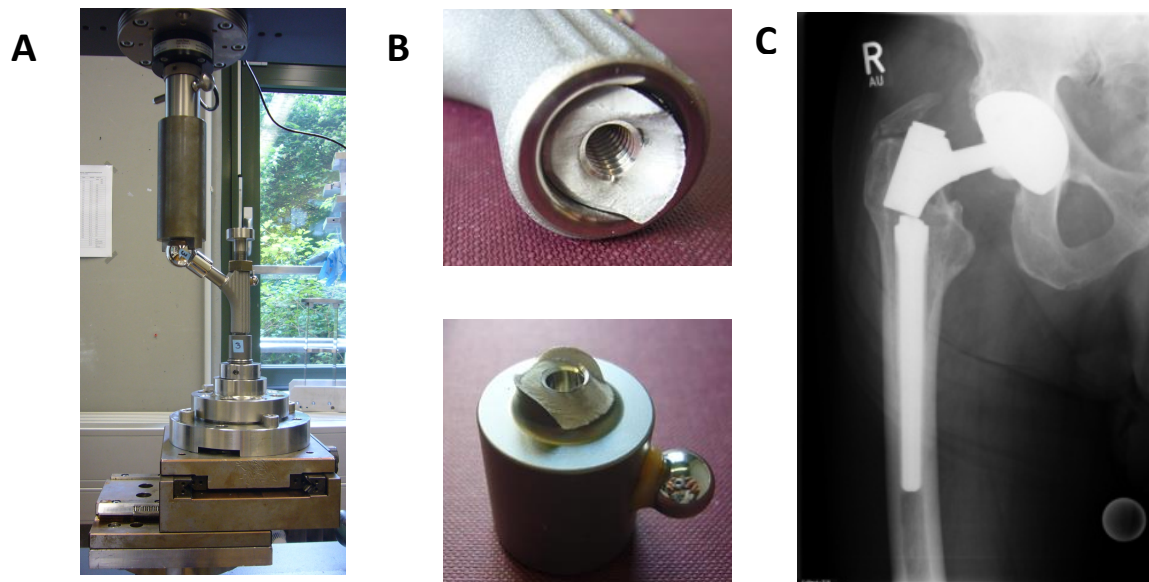
265

266 **Figure 6:** Total surface damage of the taper interface of the distal stem for varied taper
 267 diameter (8 mm - 16 mm) with a constant outside diameter of 20 mm, an
 268 assembly force of 11.0 kN for the peak force of physiological gait loading. Design c
 269 is the clinically available implant design.

270 **Validation**

271 Experimental failure testing (Figure 7A) resulted in a mean fracture load of 5.65 ± 0.61 kN,
 272 with initiation of the crack observed at the lateral side of the distal stem taper (Figure 7B),
 273 similar to the location of the highest values of bending stress of the FE-calculation and
 274 likewise comparable to in-vivo fracture images of the taper junction of modular revision

275 prosthesis (Figure 7C) and likewise comparable to in-vivo fracture images of the taper
 276 junction of modular revision prosthesis (Figure 7C). The failure force predicted for the
 277 analytical bending model was 6.06 kN, which is an overestimation of less than 8 %.

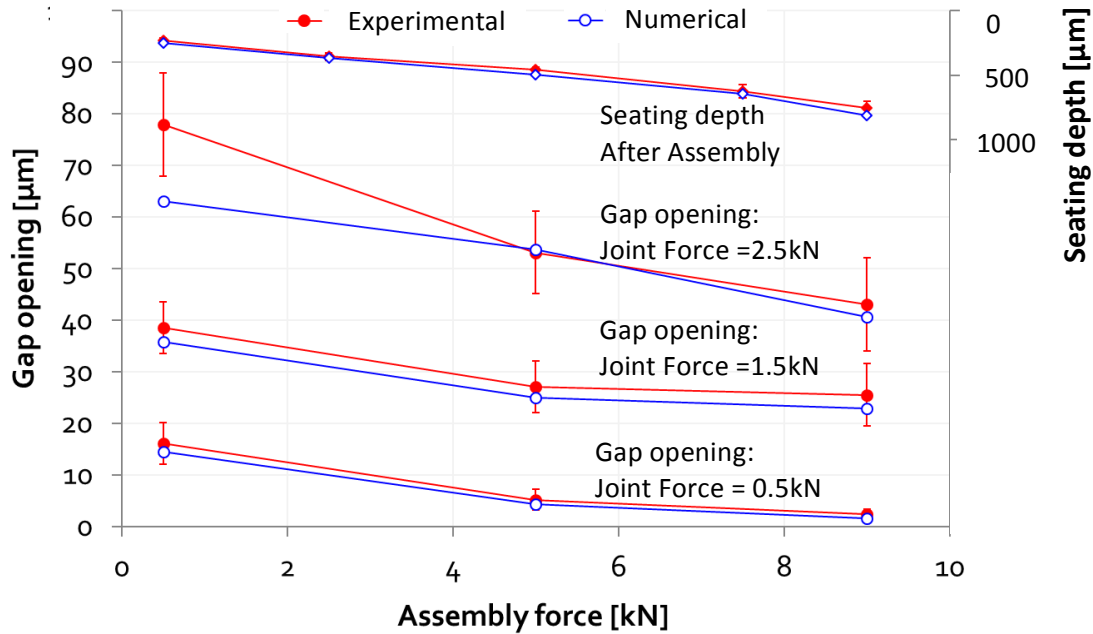


278
 279 **Figure 7:** **A:** Experimental setup for the determination of the fracture load of the distal stem
 280 taper;
 281 **B:** Fracture surfaces of the male taper;
 282 **C:** X-ray of a fractured taper junction of a modular revision hip system [65].

283 Lateral gap opening increased with applied joint force and decreased with assembly force
 284 similarly for the numerical model and the experiment (Figure 8). A maximum gap opening of
 285 $86.1 \pm 11.1 \mu\text{m}$ was measured for 0.5 kN assembly force and a joint force of 2.5 kN. The mean
 286 absolute error for the gap opening was highest for the lowest assembly force with the
 287 highest joint force (21 %). For all other combinations the error was less than 7 %.

288 The seating depth of the taper increased with increasing assembly force similarly for the
 289 model calculations and the experimental measurements (Figure 8). Seating depths of
 290 $231 \pm 20 \mu\text{m}$ and $754 \pm 55 \mu\text{m}$ were measured for assembly forces of 0.5 kN and 9.0 kN,
 291 respectively. The mean difference between calculated and measured seating depth
 292 magnitudes was between 3 % and 8 %.

293



294

295 **Figure 8:** Comparison of experimental and numerical results (FE-model) for gap opening and
 296 seating depth between the proximal neck piece and the distal stem for varying
 297 assembly forces and joint force.

298 **Discussion**

299 In this study various implant design factors, as well as surgeon and patient factors were
 300 investigated for their potential to cause failure of modular stem taper connections of
 301 femoral revision implants.

302 *Design constraints for a revision stem*

303 Revision stems are designed to achieve stability in the femoral diaphysis to bypass regions of
 304 proximal bone loss. Their outside diameter is limited by the cross section of the medullary
 305 canal. The head offset and angle of the neck piece should be matched to the patient's
 306 anatomy to achieve a satisfactory functional outcome. Titanium alloy is used for
 307 uncemented implants due to its biocompatibility and strength. The bending model
 308 demonstrated that a solid monobloc stem can have the strength to sustain most loading
 309 situations in most patients, without proximal bone support. The diameter of the male taper
 310 must be smaller than the outside diameter of a monobloc design. A modular stem is
 311 therefore weaker, but allows stable diaphyseal fixation and appropriate geometrical
 312 reconstruction to be achieved independently in the operating theatre [37].

313 The results of the analytical model indicate that problems with modular implants can occur
314 for higher loading of heavy patients, a phenomenon for which is anecdotal clinical evidence
315 [19,38,39]. Larger patients are associated with higher joint loading as well as higher neck
316 offsets. Of all the factors investigated in this study, increasing the taper diameter was shown
317 to provide the greatest advantage, since implant strength increases with the cube of the
318 diameter. This might be a solution for patients with a medullary canal that is sufficiently
319 large to accommodate an increased stem diameter.

320 The male taper diameter could also be increased for a given canal diameter by decreasing
321 the wall thickness of the (outer) female taper. The numerical simulation showed that this
322 would increase the relative motion and surface damage at the interface. Interestingly, the
323 minimum relative motion and surface damage were observed for the wall thickness of
324 current clinical designs. An alternative solution would be the use a monobloc implant (no
325 taper connection), for which the outside diameter determines the bending strength. This
326 solution was shown to be sufficiently strong for most patients undertaking normal activities.

327 The maximum bending stress generated is proportional to the lever arm of the joint force.
328 The joint force angle remains rather constant in the femoral (or stem) coordinate system
329 during a gait cycle and for other activities, suggesting that the vulnerable taper connection
330 could be positioned in the area where it intersects with the joint force vector, thus
331 minimizing the lever arm and the risk of failure. In current designs the modular taper lies
332 above this position. For the minimum head offset design the position would need to lie
333 28 mm lower and for the maximum head offset 74 mm lower than current designs.
334 However, these geometries would be impractical as they would interfere with the
335 diaphyseal anchorage of the stem.

336 Other factors influencing the mechanical failure of modular revision stems are related to the
337 patient and to the surgeon. If the patient is heavy and/or requires a high offset neck but has
338 a small endosteal diameter, and if a larger diameter taper is not available, the restriction of
339 activities or even weight loss would be indicated [54-56]. It is doubtful whether such advice
340 to patients would be practical.

341 One of the surgeon factors investigated in the current study was the assembly force applied
342 over the taper connection. This does not affect the immediate post-operative strength of the
343 stem but rather the loss of taper strength with time, by accelerating and accentuating the

344 fatigue process of the material. Fatigue is inevitable and will reduce the strength of the
345 material by 10 % at just 10^5 cycles (less than one year of standard post-operative activity)
346 and approaches a limit of 20 % reduction at 10^7 cycles (~a few years, depending on age and
347 activity) [40–42]. The influence of corrosion on implant failure is currently undergoing
348 extensive research for the head-stem junction [43–46]. Corrosion of titanium-titanium
349 modular connections has led to clinical failure by accentuated fatigue [47] and by a loss of
350 strength due to a transition of the bulk metal to the crumbly oxide [48]. In the current study
351 this effect was investigated for the stem taper, which is subjected to a larger bending
352 moment than the head-stem taper. The magnitudes of motion simulated at this interface
353 support the suggestion that fretting corrosion is likely to occur at this interface. Assuming
354 that the combination of relative shear motion and contact pressure causes surface damage,
355 maximum surface damage was observed during heel strike and toe off, where the rates of
356 change of loading are maximum (Figure 5B). The integration of relative surface damage over
357 a whole gait cycle was an order of magnitude higher for the low assembly force (0.5 kN) than
358 for the manufacturer’s suggested magnitude (11.0 kN). Application of a very large assembly
359 force (40.0 kN) reduced total surface damage by a further 8 % but high local magnitudes
360 were still observed. Therefore, increasing the assembly force may not completely eliminate
361 local fretting.

362 Corrosion can only occur in a fluid environment [49–52]. The gap opening measured in the
363 current study could allow joint fluid to enter the interface. On the other hand, runaway
364 crevice corrosion occurs in relatively stagnant fluid conditions, in which the fluid becomes
365 increasingly acidic and corrosive [51]. Fluid can permeate the interface without any loading,
366 regardless of the assembly force, due to the surface roughness (unpublished data), so that
367 gap opening may have little further impact.

368 *Limitations*

369 The analytical and numerical models presented were shown to be valid representations of
370 similar experimental models. However, various factors were neglected that may influence
371 clinical implant performance. Neglecting proximal bone support represents worst case taper
372 loading, but may represent clinical reality [57-60]. Stumbling also represents worst case
373 loading. It is unknown how frequently this occurs [61,62].

374 The strength of the pristine and fatigued material without corrosion is well defined but
375 further loss of strength due to corrosion is difficult to measure. Corrosion in titanium
376 modular connections between head and stem has been observed to lead to material loss as
377 the titanium is converted to a crumbly oxide [48]. This has not yet been reported for revision
378 stems, but their fatigue is apparently accentuated by surface corrosion, which roughens the
379 surface and facilitates crack initiation [13,45-47].

380 A single implant design was used as a template in the current study. Many of the implants
381 available have a similar geometry, due to their constraint by anatomical geometry. The
382 implant used would therefore seem to be representative of other implants.

383 *Conclusions*

384 This study addressed revision implantation without any proximal bone support around the
385 neck piece. For this situation the mechanical limits of modular revision implants can be
386 exceeded, particularly after some time in the body, and in larger patients. Since a voluntary
387 reduction of implant loading by the restriction of activities or by weight loss is difficult to
388 ensure, a larger diameter implant or a monobloc design should be considered in order to
389 increase implant strength. This would require a greater inventory in the hospital and might
390 be restricted to specialized centres. Increasing the assembly force was shown to increase the
391 contact pressure and decrease the relative interface motion. However, an increased
392 assembly force does not eliminate local wear or fretting entirely, demonstrating that any
393 taper junction can carry the risk of corrosion.

394

395 **Funding:**

396 **Ethical approval:**

397 Annika Krull, has declared no conflict of interest. Michael M. Morlock, reports personal fees
398 from DePuy Synthes, Zimmer, Ceramtec, Smith & Nephew, Aesculap and Corin; grants from
399 DePuy Synthes and Ceramtec outside the work. Nicholas E. Bishop, reports personal fees
400 from DePuy Synthes outside the work.

401 **Acknowledgments:**

402 The authors would like to thank Peter Brehm GmbH (Weissendorf, Germany) for providing
403 materials.

404 **Author's contribution:**

405 We confirm that the article is original, that all authors were involved in the study design,
406 data collection, data analysis and writing; the paper has not been submitted to any other
407 journal.

408

409

410 **References**

- 411
- 412 [1] Kurtz S, Mowat F, Ong K, Chan N, Lau E, Halpern M. Prevalence of primary and
413 revision total hip and knee arthroplasty in the United States from 1990 through 2002.
414 The Journal of bone and joint surgery. American volume 2005;87(7):1487–97,
415 doi:10.2106/JBJS.D.02441.
- 416 [2] Berry DJ. American Joint Replacement Registry 2016.
- 417 [3] Canadian Institute for Health Information / Institut canadien d'information sur la
418 santé. Canadian Joint Replacement Registry Annual Report 2015.
- 419 [4] Australian Orthopaedic Association. National joint replacement registry. Revision hip
420 and knee arthroplasty. Supplementary report 2016.
- 421 [5] Graves S. National Joint Replacement Registry, Hip Knee & Shoulder Arthroplasty,
422 Annual Report 2016.
- 423 [6] Green M, Howard PW, Porter M, Price A, Wilkinson JM, Wishart N. National
424 Joint Registry for England, Wales, Northern Ireland and the Isle of Man, 13th
425 Annual Report 2016.
- 426 [7] Grumberg A, Jansson V., Liebs T, Melsheimer O, Steinbruck A. Endoprothesenregister
427 Deutschland (EPRD) 2015.
- 428 [8] Overgaard S. Dansk Hoftaaloplastik Register - National arsrapport 2016.
- 429 [9] Röder C, Staub Lucas P. Jahresbericht 2014 Schweizerisches Hüft- und
430 Knieimplantatregister. PrimaryCare (de);15(14). p. 234–235, doi:10.4414/pc-
431 d.2015.01082.
- 432 [10] Rothwell A. The new zealand joint registry 2016.
- 433 [11] Egan KJ, Di Cesare PE. Intraoperative complications of revision hip arthroplasty using
434 a fully porous-coated straight cobalt—chrome femoral stem. The Journal of
435 Arthroplasty 1995;10:S45-S51, doi:10.1016/S0883-5403(05)80230-X.
- 436 [12] Bobynd JD, Tanzer M, Krygier JJ, Dujovne AR, Brooks CE. Concerns with modularity in
437 total hip arthroplasty. Clin Orthop Relat Res 1994(298):27–36.
- 438 [13] Atwood SA. Corrosion-Induced Fracture of a Double-Modular Hip Prosthesis. J Bone
439 Joint Surg Am 2010;92(6), doi:10.2106/JBJS.I.00980.
- 440 [14] Efe T, Schmitt J. Analyses of prosthesis stem failures in noncemented modular hip
441 revision prostheses. The Journal of Arthroplasty 2011;26(4):665,
442 doi:10.1016/j.arth.2010.05.020.
- 443 [15] Ceretti M, Falez F. Modular titanium alloy neck failure in total hip replacement:
444 Analysis of a relapse case. SICOT-J 2016;2:20, doi:10.1051/sicotj/2016009.
- 445 [16] Fink B, Urbansky K, Schuster P. Midterm results with the curved modular tapered,
446 fluted titanium Revitan stem in revision hip replacement. The Bone & Joint Journal
447 2014;96-B(7):889–95, doi:10.1302/0301-620X.96B7.33280.
- 448 [17] Konan S, Garbuz DS, Masri BA, Duncan CP. Modular tapered titanium stems in
449 revision arthroplasty of the hip: The Risk and Causes of Stem Fracture. The Bone &
450 Joint Journal 2016;98-B(1 Suppl A):50–53, doi:10.1302/0301-620X.98B1.36442.

- 451 [18] Lakstein D, Eliaz N, Levi O, Backstein D, Kosashvili Y, Safir O, Gross AE. Fracture of
452 cementless femoral stems at the mid-stem junction in modular revision hip
453 arthroplasty systems. *The Journal of bone and joint surgery. American volume*
454 2011;93(1):57–65, doi:10.2106/JBJS.I.01589.
- 455 [19] Wroblewski BM. The mechanism of fracture of the femoral prosthesis in total hip
456 replacement. *International Orthopaedics (SICOT)* 1979;3:137–39.
- 457 [20] Van Houwelingen, Andrew P, Duncan CP, Masri BA, Greidanus NV, Garbuz DS. High
458 survival of modular tapered stems for proximal femoral bone defects at 5 to 10 years
459 follow up. *Clinical Orthopaedics and Related Research* 2013;471(2):454–62,
460 doi:10.1007/s11999-012-2552-8.
- 461 [21] Cooper HJ, Della Valle CJ, Berger RA, Tetreault M, Paprosky WG, Sporer SM, Jacobs JJ.
462 Corrosion at the Head-Neck Taper as a Cause for Adverse Local Tissue Reactions After
463 Total Hip Arthroplasty. *The Journal of Bone and Joint Surgery* 2012;94(18):1655–61,
464 doi:10.2106/JBJS.K.01352.
- 465 [22] Hoberg M, Konrads C, Engelin J, Oschmann D, Holder M, Walch M, Rudert M.
466 Outcome of a modular tapered uncemented titanium femoral stem in revision hip
467 arthroplasty. *Int Orthop.* 2015(39,9):1709–13, doi: 10.1007/s00264-015-2699-5.
- 468 [23] Wright G, Sporer S, Urban R, Jacobs J. Fracture of a modular femoral neck after total
469 hip arthroplasty: A case report. *The Journal of bone and joint surgery. American*
470 *volume* 2010;92(6):1518–21, doi:10.2106/JBJS.I.01033.
- 471 [24] Norman P, Iyengar S, Svensson I, Flivik G. Fatigue fracture in dual modular revision
472 total hip arthroplasty stems: failure analysis and computed tomography diagnostics
473 in two cases. *The Journal of Arthroplasty* 2014;29(4):850–55,
474 doi:10.1016/j.arth.2013.09.008.
- 475 [25] Masri BA, Meek RMD, Duncan CP. Periprosthetic Fractures Evaluation and Treatment.
476 *Clinical Orthopaedics and Related Research* 2004;420:80–95, doi:10.1097/00003086-
477 200403000-00012.
- 478 [26] Gilbert JL, Buckley CA, Jacobs JJ. In vivo corrosion of modular hip prosthesis
479 components in mixed and similar metal combinations. The effect of crevice, stress,
480 motion, and alloy coupling. *J. Biomed. Mater. Res.* 1993;27(12):1533–44,
481 doi:10.1002/jbm.820271210.
- 482 [27] Mroczkowski ML, Hertzler JS, Humphrey SM, Johnson T, Blanchard CR. Effect of
483 impact assembly on the fretting corrosion of modular hip tapers. *Journal of*
484 *orthopaedic research official publication of the Orthopaedic Research Society*
485 2006;24(2):271–79, doi:10.1002/jor.20048.
- 486 [28] Rehmer A, Bishop NE, Morlock MM. Influence of assembly procedure and material
487 combination on the strength of the taper connection at the head–neck junction of
488 modular hip endoprostheses. *Clinical Biomechanics* 2012;27(1):77–83,
489 doi:10.1016/j.clinbiomech.2011.08.002.
- 490 [29] Bergmann G, Deuretzbacher G, Heller M, Graichen F, Rohlmann A, Strauss J, Duda G.
491 Hip contact forces and gait patterns from routine activities. *Journal of Biomechanics*
492 2001;34(7):859–71, doi:10.1016/S0021-9290(01)00040-9.

- 493 [30] Wharton MH, Waterhouse RB. Environmental effects in the fretting fatigue of Ti-6Al-
494 4V. *Wear* 1980;62(2):287–97, doi:10.1016/0043-1648(80)90174-X.
- 495 [31] Virtanen S, Milosev I, Gomez-Barrena E, Trebse R, Salo J, Konttinen YT. Special modes
496 of corrosion under physiological and simulated physiological conditions. *Acta*
497 *Biomaterialia* 2008;4(3):468–76, doi:10.1016/j.actbio.2007.12.003.
- 498 [32] Hoepfner DW, Chandrasekaran V. Fretting in orthopaedic implants: A review. *Wear*
499 1994;173(1-2):189–97, doi:10.1016/0043-1648(94)90272-0.
- 500 [33] Budinski KG. Tribological properties of titanium alloys. *Wear* 1991;151(2):203–17.
- 501 [34] Swaminathan V, Gilbert JL. Potential and frequency effects on fretting corrosion of
502 Ti6Al4V and CoCrMo surfaces. *Journal of biomedical materials research. Part A*
503 2013;101(9):2602–12, doi:10.1002/jbm.a.34564.
- 504 [35] Archard JF. Contact and Rubbing of Flat Surfaces. *Journal of Applied Physics*
505 1953;24(8):981–88, doi:10.1063/1.1721448.
- 506 [36] Archard JF, Hirst W. The Wear of Metals under Unlubricated Conditions. *Proceedings*
507 *of the Royal Society A: Mathematical, Physical and Engineering Sciences*
508 1956;236(1206):397–410, doi:10.1098/rspa.1956.0144.
- 509 [37] Frye BM, Berend KR, Morris MJ, Adams JB, Lombardi AV. Modular Femoral Tapered
510 Revision Stems in Total Hip Arthroplasty. *Joint Implant Surgery & Research*
511 *Foundation - Reconstructive Review* 2013;3(4):32–37.
- 512 [38] Skendzel JG, Blaha JD, Urquhart AG. Total hip arthroplasty modular neck failure. *The*
513 *Journal of Arthroplasty* 2011;26(2):338, doi:10.1016/j.arth.2010.03.011.
- 514 [39] Busch CA, Charles MN, Haydon CM, Bourne RB, Rorabeck CH, Macdonald SJ,
515 McCalden RW. Fractures of distally-fixed femoral stems after revision arthroplasty.
516 *The Journal of bone and joint surgery. British volume* 2005;87(10):1333–36,
517 doi:10.1302/0301-620X.87B10.16528.
- 518 [40] Morlock MM, Schneider E, Bluhm A, Vollmer M, Bergmann G, Müller V, Honl M.
519 Duration and frequency of every day activities in total hip patients. *Journal of*
520 *Biomechanics* 2001;34(7):873–81, doi:10.1016/S0021-9290(01)00035-5.
- 521 [41] Wallbridge N, Dowson D. The walking activity of patients with artificial hip joints.
522 *Engineering in medicine* 1982;11(2):95–96.
- 523 [42] Schmalzried TP, Szuszczewicz ES, Northfield MR, Akizuki KH, Frankel RE, Belcher G,
524 Amstutz HC. Quantitative assessment of walking activity after total hip or knee
525 replacement. *J Bone Joint Surg Am* 1998;80(1):54–59.
- 526 [43] Hussenbocus S, Kosuge D, Solomon LB, Howie DW, Oskouei RH. Head-neck taper
527 corrosion in hip arthroplasty. *BioMed Research International* 2015;2015:758123,
528 doi:10.1155/2015/758123.
- 529 [44] Morlock MM, Bunte D, Ettema H, Verheyen CC, Hamberg A, Gilbert J. Primary hip
530 replacement stem taper fracture due to corrosion in 3 patients. *Acta orthopaedica*
531 2016;87(2):189–92, doi:10.3109/17453674.2015.1128780.
- 532 [45] Weiser MC, Chen DD. Revision for taper corrosion at the neck-body junction
533 following total hip arthroplasty: Pearls and pitfalls. *Current reviews in*
534 *musculoskeletal medicine* 2016;9(1):75–83, doi:10.1007/s12178-016-9322-2.

- 535 [46] Munir S, Cross MB, Esposito C, Sokolova A, Walter WL. Corrosion in modular total hip
536 replacements: An analysis of the head–neck and stem–sleeve taper connections.
537 *Seminars in Arthroplasty* 2013;24(4):240–45, doi:10.1053/j.sart.2014.01.009.
- 538 [47] Grupp TM, Weik T, Bloemer W, Knaebel H-P. Modular titanium alloy neck adapter
539 failures in hip replacement--failure mode analysis and influence of implant material.
540 *BMC musculoskeletal disorders* 2010;11:3, doi:10.1186/1471-2474-11-3.
- 541 [48] Witt F, Bosker BH, Bishop NE, Ettema HB, Verheyen, C. C. P. M., Morlock MM. The
542 Relation Between Titanium Taper Corrosion and Cobalt-Chromium Bearing Wear in
543 Large-Head Metal-on-Metal Total Hip Prostheses: A Retrieval Study. *The Journal of*
544 *Bone & Joint Surgery* 2014;96(18):e157-e157, doi:10.2106/JBJS.M.01199.
- 545 [49] Chu Y-H, Elisa J, Duda G, Frassica F, Chao E. Stress and micromotion in the taper lock
546 joint of a modular segmental bone replacement prosthesis. *Journal of Biomechanics*
547 2000;33:1175–79.
- 548 [50] Del Balso C, Teeter MG, Tan SC, Howard JL, Lanting BA. Trunnionosis: Does Head Size
549 Affect Fretting and Corrosion in Total Hip Arthroplasty? *The Journal of Arthroplasty*
550 2016, doi:10.1016/j.arth.2016.03.009.
- 551 [51] Gilbert JL, Mali S, Urban RM, Silverton CD, Jacobs JJ. In vivo oxide-induced stress
552 corrosion cracking of Ti-6Al-4V in a neck-stem modular taper: Emergent behavior in a
553 new mechanism of in vivo corrosion. *J. Biomed. Mater. Res. Part B Appl. Biomater.*
554 2011, doi:10.1002/jbm.b.31943.
- 555 [52] Lieberman JR, Rimnac CM, Garvin KL, Klein RW, Salvati EA. An analysis of the head-
556 neck taper interface in retrieved hip prostheses. *Clin. Orthop. Relat. Res.*
557 1994(300):162–67.
- 558 [53] ASTM F67 Grade 4; Unalloyed Titanium for Surgical Implant Application, 2013.
- 559 [54] Meller MM, Toossi N, Gonzalez MH, Son MS, Lau EC, Johanson N. Surgical Risk and
560 Costs of Care are Greater in Patients Who Are Super Obese and Undergoing THA. *Clin*
561 *Orthop Relat Res.* 2016(474):2472-84, doi: 10.1007/s11999-016-5039-1.
- 562 [55] Traina F, Bordini B, De Fine M, Toni A. Patient weight more than body mass index
563 influence total hip arthroplasty long term survival. *Hip Int.* 2011(21,6):694-9, doi:
564 10.5301/HIP.2011.8879.
- 565 [56] Haverkamp D, Klinkenbijn MN, Somford MP, Albers GH, van der Vis HM. Obesity in
566 total hip arthroplasty – does it really matter? A meta-analysis. *Acta Orthop.*
567 2011(82,4):417-22, doi: 10.3109/17453674.2011.588859.
- 568 [57] Viste A, Perry KI, Taunton MJ, Hanssen AD, Abdel MP. Proximal femoral replacement
569 in contemporary revision total hip arthroplasty for severe femoral bone loss. *Bone*
570 *Joint J.* 2017(99-B):325-9, doi: 10.1302/0301-620X.99B3.BJJ-2016-0822.R1.
- 571 [58] Amanatullah DF, Howard JL, Siman H, Trousdale RT, Mabry TM, Berry DJ. Revision
572 total hip arthroplasty in patients with extensive proximal femoral bone loss using a
573 fluted tapered modular femoral component. *Bone Joint J.* 2015(97-B):312-7, doi:
574 10.1302/0301-620X.97B3.34684.
- 575 [59] Dzaja I, Lyons MC, McCalden RM, Naudie DD, Howard JL. Revision hip arthroplasty
576 using a modular revision hip system in case of severe bone loss. *J Arthroplasty.* 2014
577 (29,8):1594-7, doi: 10.1016/j.arth.2014.02.035.

- 578 [60] Bischel OE, Böhm PM. The use of a femoral revision stem in the treatment of primary
579 or secondary bone tumors of the proximal femur: a prospective study of 31 cases. *J*
580 *Bone Joint Surg Br.* 2010(92,10):1435-41, doi: 10.1302/0301-620X.92B10.24024.
- 581 [61] Graham DF, Modenese L, Trewartha G, Carty CP, Constantinou M, Lloyd DG, Barrett
582 RS. Hip joint contact loads in older adults during recovery from forward loss of
583 balance by stepping. *J Biomech.* 2016(49,13):2619-24, doi:
584 10.1016/j.jbiomech.2016.05.033.
- 585 [62] Bergmann G, Graichen F, Rohlmann A. Hip joint contact forces during stumbling.
586 *Langenbecks Arch Surg.* 2004(389,1):53-9, doi: 10.1007/s00423-003-0434-y.
- 587 [63] Timoshenko S. *Strength of Materials: Part I, Elementary Theory and Problems*, 3d
588 ed. D. Van Nostrand Co., New York, 1955. 442.
- 589 [64] Australian Orthopaedic Association. National joint replacement registry. Revision hip
590 and knee arthroplasty. Supplementary report 2017.
- 591 [65] Brehm, P.; internal document, 2015.
- 592